Nuclear Engineering and Technology 57 (2025) 103408

Contents lists available at ScienceDirect

Nuclear Engineering and Technology

journal homepage: www.elsevier.com/locate/net

Original Article

# An optimal procedure for fragility analysis of nuclear containment structures under internal pressure

Hoang D. Nguyen [a], Chanyoung Kim [b], Myoungsu Shin [b,*]

[a] Department of Civil and Environmental Engineering, Faculty of Engineering, University of Alberta, Edmonton, Alberta, T6G 1H9, Canada
[b] Department of Civil, Urban, Earth, and Environmental Engineering, Ulsan National Institute of Science and Technology (UNIST), 50 UNIST-gil, Ulsan, Republic of Korea

ARTICLE INFO

*Keywords:*
Nuclear power plants
Nuclear containment structures
Pressure analysis
Fragility analysis
Optimal procedure
Nuclear safety

ABSTRACT

This study aims to develop a novel efficient procedure for determining the fragility function of nuclear containment structures under internal pressure. This procedure can substantially reduce the computational cost by optimizing the required number of nonlinear structural analyses, which is initially unclear in the pressure fragility analysis. The core principle of the proposed procedure is to monitor the changes of the mean ($P_m$) and standard deviation ($\beta_S$) of ultimate pressure at failure while gradually increasing the number of structural analyses. The process is terminated when the changes in $P_m$ and $\beta_S$ between two consecutive steps drop below a prescribed threshold. The proposed procedure was applied to the pressure fragility analysis of an existing type of containment structure. Since the proposed procedure involves the random selection of additional value sets of the uncertainty parameters at each step, it was repeated 10 times to ensure a fair evaluation. The fragility curve obtained from as small as 40 analyses was nearly identical to that from 100 analyses. On average, over the 10 repeated cases, the computation time was reduced by approximately 47 % compared to the case of 100 analyses. The results confirm that the proposed procedure not only significantly reduced the computational demand but also ensured the reliable generation of the pressure fragility function.

## 1. Introduction

Fragility analysis of nuclear containment structures under internal pressure is a critical procedure to evaluate nuclear safety and engineering. It involves assessing the probability of failure of containment structures due to internal pressure loads that might occur during severe accident conditions. Containment structures are important components of nuclear power plants, designed specifically to enclose radioactive materials in the case of an accident, thereby preventing their release into the environment [1]. Particularly after the 2011 Fukushima earthquake in Japan, the safety of containment structures under internal pressure has been the subject of extensive research worldwide [1–4].

Several studies related to the safety of nuclear containment structures under internal pressure are noteworthy. Huang et al. [5] evaluated the performance of a containment structure under both service load and a hypothetical beyond-design level internal pressure. Hu et al. [6] developed a numerical model to estimate the ultimate pressure capacity and the failure mode of a prestressed concrete containment, later extending their research to include long-term prestressing loss [7]. Wang [8] formulated an analytical model for the dome-cylinder interface of a nuclear containment, focusing on its response to internal pressure and thermal load. However, these studies predominantly employed deterministic analysis methods, without considering uncertainties in material properties (e.g., rebar, concrete), boundary conditions, or loading inputs (e.g., prestress).

In conducting the pressure fragility analysis of containment structures, the probabilistic method has been widely adopted [9–12]. This methodology involves performing numerous nonlinear structural analyses under the influence of uncertainty parameters such as concrete or rebar properties, which are selected and generated using the Monte Carlo simulation [13] and/or Latin Hypercube sampling (LHS) [14]. The main concern in this context is determining the optimal number of samples for uncertainty parameters (i.e., the number of pressure analyses) that should be generated to ensure accuracy and computational efficiency. The numerical model of a nuclear containment structure is sophisticated [15], leading to a substantial computational demand for each analysis. This is especially true in the pressure analysis, where the internal pressure is increased until the containment structure reaches

* Corresponding author.
*E-mail address:* msshin@unist.ac.kr (M. Shin).

https://doi.org/10.1016/j.net.2024.103408
Received 30 April 2024; Received in revised form 18 November 2024; Accepted 22 December 2024
Available online 24 December 2024

the specified failure criteria (e.g., the maximum strain of steel liner plate, tendon, rebar, or concrete).

In previous studies on the pressure fragility analysis of nuclear containments, Barbat et al. [16] used 100 samples through the Monte Carlo method to establish the probability density curve of ultimate pressure at failure that was used to derive the fragility curve, assuming the ultimate pressure follows the normal distribution. Zhou et al. [9] also generated 100 samples for the main materials of a containment structure using the Monte Carlo simulation to develop the fragility function of the structure subjected to internal pressure. Meanwhile, the Korea Atomic Energy Research Institute (KAERI) [17] employed the Monte Carlo simulation with LHS to generate 30 sets of uncertainty parameters, and used them to estimate the ultimate pressures and develop the fragility curve. Jin and Gong [10] explored the impact of varying sample sizes - 100, 500, and 1000, generated using the Monte Carlo simulation with LHS - on the fragility curves of containment structures under internal pressure.

It can be observed that there is no solid principle for selecting the number of samples for the pressure fragility analysis of nuclear containments using the probabilistic method. An optimal number of nonlinear structural analyses could significantly reduce the computational cost in this method. Given that, this study aims to address this research gap by proposing a novel efficient procedure to determine the optimal number of numerical analyses for the generation of the pressure fragility function. Specifically, this procedure monitors the changes in two critical parameters (i.e., the median and logarithmic standard deviation of ultimate pressure) that define the fragility curve, while increasing the number of numerical analyses stepwise. To demonstrate the efficacy of the proposed procedure, we applied it to the pressure fragility analysis of an existing type of containment structure.

The structure of this paper is outlined as follows. Section 2 presents the background research on probabilistic analysis methods. Section 3 introduces the proposed procedure for the fragility analysis of nuclear containment structures subjected to internal pressure. The implementation of the proposed procedure through a case study of a containment structure is demonstrated in Section 4. Finally, the principal findings derived from this research are discussed in Section 5.

## 2. Probabilistic method for pressure fragility analysis of nuclear containment structures

In general, the probabilistic analysis methodology is used to examine the fragility analysis of nuclear containment structures against internal pressure. This approach can be divided into six essential steps outlined in the following.

**Step 1 - Development of structural model:** This initial step involves the development of a detailed structural model that represents specific characteristics and complexities of the nuclear containment structure.

**Step 2 - Selection of uncertainty parameters and generation of samples**: In this step, key uncertainty parameters, such as the properties of concrete and steel, are selected. Then, $n$ different value sets (i.e., samples) of the parameters are generated. Generally, the Monte Carlo simulation, occasionally combined with LHS, is used to generate the samples for uncertainty parameters.

**Step 3 - Definition of failure criteria**: This critical step involves defining the failure criteria for nuclear containment structures under internal pressure. The failure criterion is assigned to an engineering demand parameter (EDP) and its threshold (e.g., the strain of rebars with a threshold of 0.8 % or the strain of tendons with a threshold of 0.8 % [18]).

**Step 4 - Determination of ultimate pressure**: The ultimate pressure is determined when the containment structure reaches the defined failure criteria. Ultimate pressure values are determined for $n$ value sets of uncertainty parameters, i.e., $n$ different analyses.

**Step 5 - Calculation of input parameters for constructing the fragility curve**: This step involves determining the median ($P_m$) and logarithmic standard deviation ($\beta_S$) of the $n$ different ultimate pressures of containment structures, utilizing Eq. (1) and Eq. (2) respectively.

**Step 6 - Construction of fragility curve:** The final step involves developing the fragility curve using Eq. (3), where $P(p)$ represents the probability of failure due to the internal pressure $p$. The fragility curve illustrates the probability of failure of nuclear containment structures at various levels of internal pressure.

$$P_m = \exp\left(\frac{1}{n}\sum_{i=1}^{n}\ln\left(P_i\right)\right) \quad \text{Eq. (1)}$$

$$\beta_S = \sqrt{\frac{1}{n-1}\sum_{i=1}^{n}\left(\ln\left(\frac{P_i}{P_m}\right)\right)^2} \quad \text{Eq. (2)}$$

$$P(p) = \Phi\left(\frac{p/P_m}{\beta_S}\right) \quad \text{Eq. (3)}$$

## 3. Proposed procedure for pressure fragility analysis of nuclear containment structures

In this study, an optimal procedure was proposed to mitigate the high computation cost for the pressure fragility analysis of nuclear containment structures. The core operation of the proposed procedure is to monitor the two main parameters (i.e., $P_m$ and $\beta_S$) that are used to construct the fragility curve based on the probabilistic method in Section 2.

Fig. 1 illustrates the main concept of the proposed procedure. The initial step, denoted as START in the figure, begins with the random selection of $m$ sets from the total $n$ value sets of uncertainty parameters; this will be discussed in detail in Section 4.2. From the numerical analyses, $m$ ultimate pressure values corresponding to the $m$ sets of uncertainty parameters are determined. Then, $P_{m0}$ and $\beta_{S0}$ are calculated using Eq. (1) and Eq. (2), respectively.

In Step 1 ($k = 1$), $i$ sets from the ($m$-$n$) remaining value sets are randomly selected, and $i$ ultimate pressure values are determined from the numerical analyses. Subsequently, $P_{m1}$ (median of ultimate pressure at Step 1) and $\beta_{S1}$ (logarithmic standard deviation of ultimate pressure at Step 1) are computed for the $m$ ultimate pressure values from the initial step plus the $i$ ultimate pressure values from Step 1. Then, the discrepancies in $P_m$ ($\epsilon_{P_{m1}}$) and $\beta_S$ ($\epsilon_{\beta_{S1}}$) between Step 1 and the initial step are checked. If both $\epsilon_{P_{m1}}$ and $\epsilon_{\beta_{S1}}$ are less than a predefined value ($\epsilon_D$), the analysis process can be terminated. Otherwise, the procedure will continue to Step 2, and it will be continued until Step $k$ where the discrepancies (i.e., $\epsilon_{P_{mk}}$ and $\epsilon_{\beta_{Sk}}$) of two consecutive steps are smaller than $\epsilon_D$. Fig. 2 illustrates the graphical description of monitoring changes in $P_m$ and $\beta_S$ to determine the required number of analyses based on the proposed procedure.

## 4. Application of proposed procedure to a case-study containment structure

### 4.1. Numerical modeling of the considered structure

This section demonstrates the efficiency of the proposed procedure by its application to a case-study structure, the APR1400 reactor containment building [19]. The numerical model of the containment structure was developed using ABAQUS software [20].

Fig. 3 shows the 3-dimensional (3D) finite element model of the considered containment structure used in this study. It consists of a cylindrical wall, a hemispherical upper dome, three vertical buttresses, a foundation slab, a liner steel plate, reinforcing bars, and prestressed tendons placed in the foundation slab, dome, and wall. The prestressed

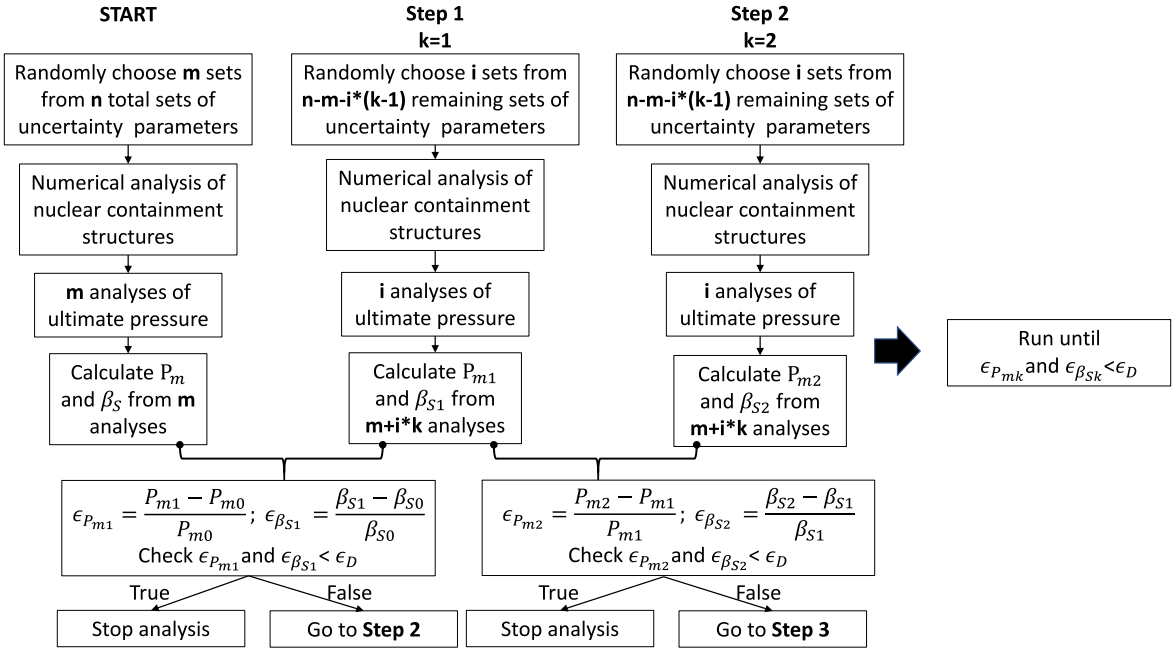


**Fig. 1.** – Schematic of the proposed procedure.

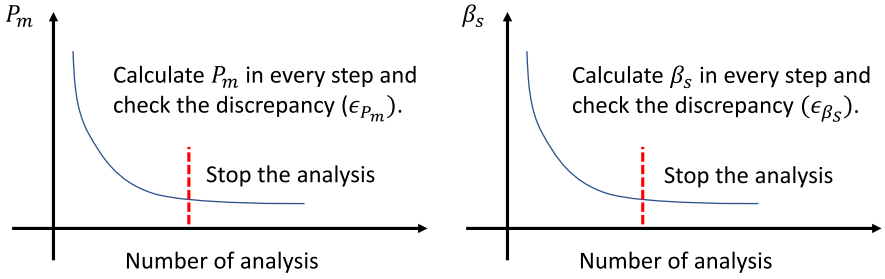


**Fig. 2.** – Illustration to determine the required number of analyses monitoring $P_m$ and $\beta_S$

tendons are embedded in both the wall and the dome, and the tendons in a hoop direction are supported by the three buttresses. Furthermore, inverted U-shaped tendons in a meridional direction, which extend across the wall and dome, are anchored within the tendon gallery of the foundation slab. Fig. 4. Shows the geometry and main components of the APR1400 reactor containment building.

The cylindrical wall has multiple penetrations, which include large-scale penetrations like an equipment hatch and personal airlock, as well as several small-scale electrical and mechanical penetrations. It was assumed that there would be no leakage from the seals around these penetrations. The cylindrical wall was modeled using six layers of solid elements in the wall-depth direction to simulate the behavior of the wall under internal pressure. The wall portion and the foundation slab portion are cast with concrete separately during construction, but reinforcing bars and prestressed tendons tie the wall and the foundation together. Moreover, prestressing forces provide additional load-carrying capacity against internal pressure. Therefore, the wall-foundation interface was assumed to be completely closed or sealed for the purpose of pressure analysis. Further details on the nuclear containment structure used in this study are available in the referenced literature [17].

The materials used in the containment structure include concrete, steel rebar, steel liner, and prestressed tendon. Table 1 summarizes the statistical characteristics of the materials considered in this study. Fig. 5 shows the uniaxial stress-strain relationships of the four materials based on their mean values. For concrete, a damaged plasticity model was employed to define the stress-strain behavior, referring to the methodology proposed by Alfarah et al. [21]. The uniaxial behavior of reinforcing bars was defined following the model proposed by Mansour and Hsu [22]. Furthermore, the behaviors of steel liner and prestressed tendons were defined in accordance with the KAERI guidelines [17].

In the finite element model in ABAQUS, the concrete members were represented by 8-noded hexahedral elements (C3D8R). The rebars and prestressed tendons were modeled with fully integrated 2-noded truss elements (T3D2), while the steel liner was modeled using 4-node quadrilateral surface elements (S4R).

Another important step in the pressure fragility analysis of nuclear containment structures is to define the failure criteria to establish the ultimate pressure. During the numerical analysis in ABAQUS, the internal pressure is statically applied over the entire liner plate, and is increased by small increments. In this study, we assumed that the ultimate pressure of a nuclear containment structure is reached when the steel liner in the global free field undertakes the maximum strain of 0.4 % on average [23]. Fig. 6 shows an example to determine the ultimate pressure corresponding to the maximum strain of 0.4 % based on the results obtained from the ABAQUS analyses under incremental internal pressures.

**Fig. 3.** – 3D ABAQUS model of the considered structure, APR1400 reactor containment building.

### 4.2. Considered uncertainty parameters

The selection of uncertainty parameters and the generation of their value sets are required for the probabilistic fragility analysis of nuclear containment structures. In this investigation, the selection of uncertainty parameters incorporated insights from previous studies [9,10,14,15]. Jin and Gong [10] and Jin et al. [11] considered 11 uncertainty parameters related to material properties for the fragility analysis and

**Table 1**
– Information on considered uncertainty parameters.

| No | Uncertainty parameter | Mean | Cov | References |
|---|---|---|---|---|
| 1 | Concrete compressive strength | 41.37 MPa | 0.15 | Jin and Gong [10] |
| 2 | Concrete tensile strength | 4.329 MPa | 0.15 | Jin and Gong [10] |
| 3 | Modulus of elasticity of concrete | 30441.7 MPa | 0.08 | Rajashekhar and Ellingwood [25] |
| 4 | Yield stress of rebar | 413 MPa | 0.05 | Zhou et at [9]. |
| 5 | Modulus of elasticity of rebar | 220 GPa | 0.03 | Rajashekhar and Ellingwood [25] |
| 6 | Yield stress of steel liner | 205 MPa | 0.05 | Zhou et at [9]. |
| 7 | Modulus of elasticity of steel liner | 220 GPa | 0.03 | Rajashekhar and Ellingwood [25] |
| 8 | Yield stress of tendon | 1297 MPa | 0.025 | Zhou et at [9]. |
| 9 | Modulus of elasticity of tendon | 196 GPa | 0.03 | Rajashekhar and Ellingwood [25] |
| 10 | Density of concrete | 2400 kg/m$^3$ | 0.03 | Balomenos and Pandey [16] |
| 11 | Density of rebar | 8050 kg/m$^3$ | 0.03 | Balomenos and Pandey [16] |
| 12 | Density of steel liner | 8050 kg/m$^3$ | 0.03 | Balomenos and Pandey [16] |
| 13 | Density of tendon | 8050 kg/m$^3$ | 0.03 | Balomenos and Pandey [16] |
| 14 | Prestressing load in horizontal direction | 850 MPa | 0.10 | KAERI [17] |
| 15 | Prestressing load in vertical direction | 1000 MPa | 0.10 | KAERI [17] |

Cov: Coefficient of variation.

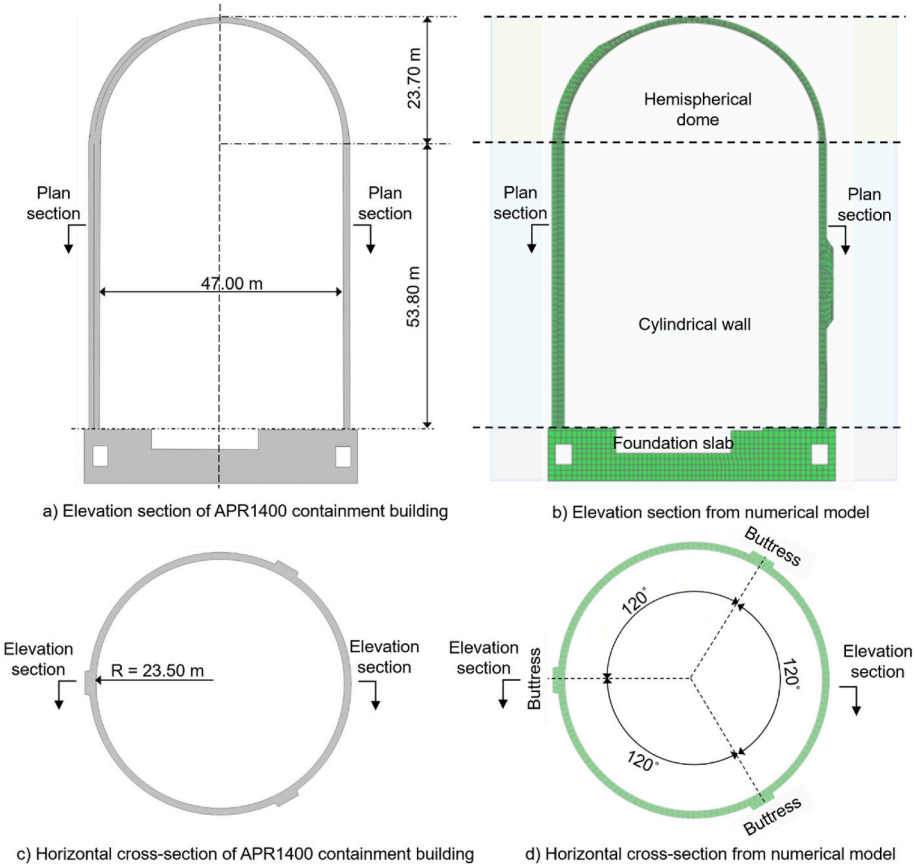


**Fig. 4.** – Geometry and main components of APR1400 reactor containment building.

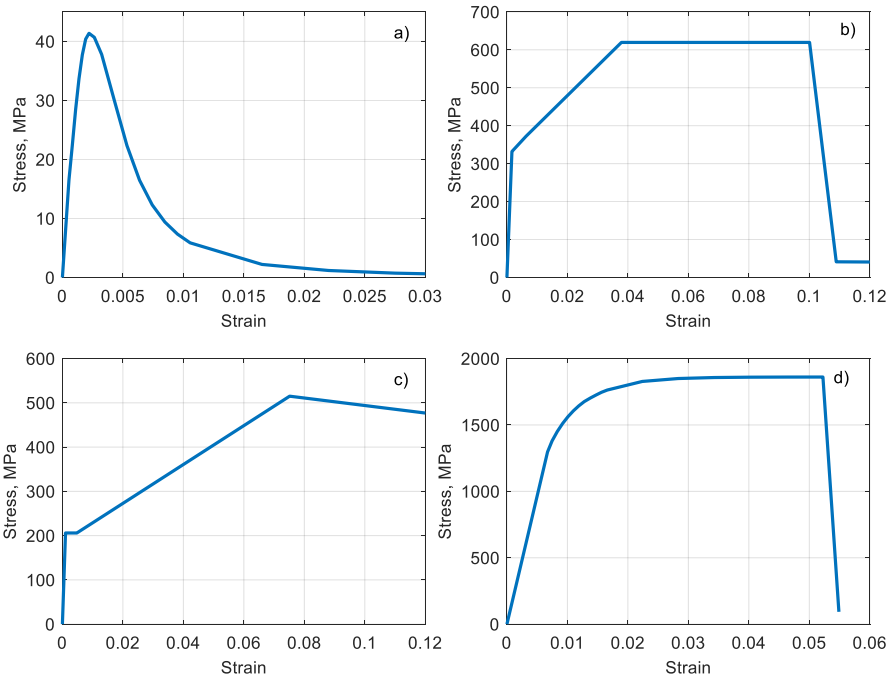


**Fig. 5.** – Normal stress-strain relationships of materials: a) concrete (in compression), b) steel rebar, c) steel linear, and d) prestressed tendon.

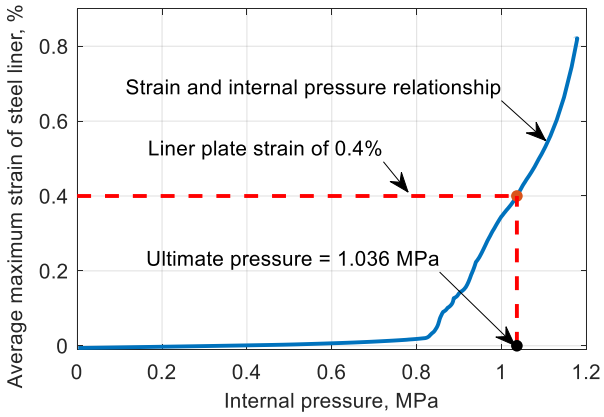


**Fig. 6.** – Example for determining the ultimate pressure.

probabilistic performance evaluation of nuclear containment structures under internal pressure. Balomenos and Pandey [16] included the densities of materials (i.e., concrete, rebar, steel liner, and tendon) as uncertainty parameters. In addition, KAERI [17] reported that the prestress loadings in both vertical and horizontal directions also greatly affect the pressure capacity of nuclear containment structures. Hence, a total of 15 uncertainty parameters in Table 1 were considered in this study. It is noted that the mean values were obtained from the report by Kwak and Kwon [24] on the APR1400 reactor containment building, and the Cov values were taken from the references listed in Table 1.

### 4.3. Fragility analysis results and discussions

Following the proposed procedure in Section 3, $n$ total value sets of uncertainty parameters should be prepared at the beginning. Jin and Gong [10] reported that differences in the fragility curves of nuclear containment structures under internal pressure, derived from 100, 500, and 1000 samples, were insignificant. Based on this finding, this study employed 100 value sets ($n = 100$ in Fig. 1) for 15 considered uncertainty parameters (Table 1) as the reference case, using Monte Carlo simulation with Latin Hypercube Sampling. At the START step, a total of 10 sets ($m = 10$ in Fig. 1) from the pool of 100 value sets were randomly selected and analyzed. In the subsequent steps, additional two sets ($i = 2$ in Fig. 1) were randomly selected and analyzed. In this study, a value of 0.5 % was used for $\epsilon_D$ to check the discrepancies between two consecutive steps (i.e., $\epsilon_{Pmk}$ and $\epsilon_{\beta_{sk}}$) and stop the analysis.

Fig. 7 displays the results acquired by the proposed procedure for a random selection case of additional value sets of the uncertainty parameters (case no. 7 in Table 2). Specifically, Fig. 7a shows the changes of $P_m$ and $\beta_S$ at each step, and indicates when the analysis was terminated. In this case, the required number of analyses was 40 ($k = 15$ in Fig. 1) for a discrepancy threshold of 0.5 %. Fig. 7b compares the fragility curve acquired by the proposed procedure (i.e., 40 analyses) with those derived from 10 to 100 analyses. The results demonstrate the high efficacy of the proposed procedure by showing that the fragility curve from 40 analyses is nearly identical to that from 100 analyses. In contrast, the fragility curve from 10 analyses is much different from that from 100 analyses.

In the case of 40 analyses, the internal pressures at failure probabilities of 5 %, 50 %, and 95 % were 0.7499 MPa, 1.1957 MPa, and 1.8840 MPa, respectively. Meanwhile, the corresponding values from 100 analyses were determined at 0.7501 MPa, 1.1527 MPa, and 1.7713 MPa, respectively. The largest difference among the three failure points was only 6.359 %, which is considered negligible. Moreover, the computation time was significantly reduced by 60 % in this specific case compared to the case of 100 analyses.

To ensure a fair evaluation, the proposed procedure was repeated 10 times using different value sets of the uncertainty parameters, as the results depended on the random selection at each step. Table 2 summarizes the required number of analyses acquired by the procedure, the internal pressures at failure probabilities of 5 %, 50 %, and 95 % determined based on the analyses, and the differences of internal pressures at the three failure probabilities between the considered case and the case of all 100 analyses. Across the 10 cases, the proposed procedure resulted in around 53 required analyses on average. In other words, the

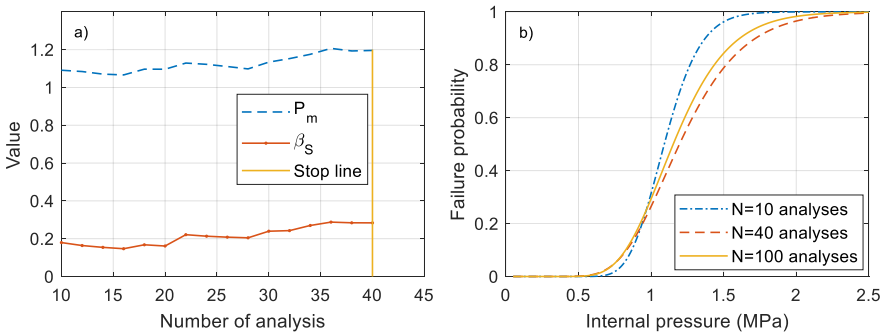


**Fig. 7.** – Fragility analysis results: a) Changes in $P_m$ and $\beta_S$, b) fragility curves based on initial 10 analyses, required 40 analyses, and all 100 analyses.

**Table 2**
– Results from the proposed procedure across 10 repeated cases.

| Case | Required number of analyses | Failure probability of 5 % | | Failure probability of 50 % | | Failure probability of 95 % | |
|---|---|---|---|---|---|---|---|
| | | Internal pressure (MPa) | Difference (%) | Internal pressure (MPa) | Difference (%) | Internal pressure (MPa) | Difference (%) |
| 1 | 48 | 0.762 | 1.539 | 1.136 | 1.480 | 1.693 | 4.415 |
| 2 | 48 | 0.763 | 1.708 | 1.170 | 1.480 | 1.793 | 1.246 |
| 3 | 50 | 0.760 | 1.285 | 1.159 | 0.515 | 1.767 | 0.248 |
| 4 | 60 | 0.741 | 1.161 | 1.174 | 1.814 | 1.858 | 4.875 |
| 5 | 68 | 0.754 | 0.472 | 1.150 | 0.260 | 1.754 | 0.996 |
| 6 | 60 | 0.750 | 0.032 | 1.129 | 2.065 | 1.699 | 4.056 |
| 7 | 40 | 0.749 | 0.027 | 1.153 | 3.730 | 1.884 | 6.359 |
| 8 | 70 | 0.734 | 2.092 | 1.167 | 1.211 | 1.853 | 4.616 |
| 9 | 44 | 0.783 | 4.368 | 1.192 | 3.409 | 1.815 | 2.451 |
| 10 | 44 | 0.748 | 0.299 | 1.160 | 0.631 | 1.799 | 1.563 |

computation time was reduced by approximately 47 % on average, compared to the case of 100 analyses. Moreover, among 10 repeated cases, the average differences of internal pressures between the considered cases and the case of all 100 analyses at failure probabilities of 5 %, 50 %, and 95 % were only 1.298 %, 1.660 %, and 3.083 %, respectively.

Of the 10 cases, the minimum required number of analyses was 40, with a variation ranging from 40 to 70 analyses. Therefore, for the initial random selection of $m$ value sets at the START step (Fig. 1), setting $m$ close to 40 would save the computational effort at the beginning, and an $i$ value (Fig. 1) of 2 is deemed appropriate.

Overall, based on these results, the proposed procedure demonstrates the potential to reduce the computational cost for the nonlinear pressure analysis of nuclear containment structures while yielding reliable results for their fragility analysis regarding internal pressure.

## 5. Conclusions

This study proposed a novel efficient procedure designed to mitigate the computational burden associated with the fragility analysis of nuclear containment structures under accidental internal pressure. The core principle of the proposed method is to progressively increase the number of analyses at each step while monitoring the changes of two critical parameters ($P_m$ and $\beta_S$) that shape the fragility curve. The analysis process is terminated once the changes in both $P_m$ and $\beta_S$ fall below a predefined threshold. The proposed procedure was applied to the pressure fragility analysis of an existing type of containment structure, the APR1400 reactor containment building. The numerical model for the containment structure was developed and analyzed using the ABAQUS software. In this application, a total of 15 uncertainty parameters comprising material (i.e., concrete, rebar, steel liner, and tendon) characteristics and prestress loading conditions were considered, and 100 value sets for them were initially generated using Monte Carlo simulation with LHS. The investigations lead to the following findings and conclusions.

- The proposed procedure not only significantly reduces the computational demand of nonlinear pressure analyses but also ensures the reliable generation of fragility functions. In the considered case study, the results demonstrate the high efficacy of the proposed procedure, showing that the fragility curve obtained from as small as 40 analyses was nearly identical to that from 100 analyses.
- For a fair evaluation, the proposed procedure was repeated 10 times using different random value sets of the uncertainty parameters, and the results were compared with those from 100 analyses. In the 10 repeated cases, the process was terminated at 40 to 70 analyses. On average, the computation time was reduced by approximately 47 % compared to the case of 100 analyses.
- Between the 10 repeated cases and the case of 100 analyses, the average differences in internal pressures corresponding to failure probabilities of 5 %, 50 %, and 95 % were only 1.298 %, 1.660 %, and 3.083 %, respectively, which are minimal.

The findings indicate that the proposed procedure has a high potential for optimizing the computational cost in the pressure fragility analysis of nuclear containment structures. However, the results of the proposed procedure may depend on the random selection of additional value sets of uncertainty parameters at each step. Hence, implementing a method (e.g., hierarchical clustering) to optimize this random selection process could enhance the effectiveness of the procedure. Furthermore, appropriate threshold values of the median and the standard deviation (i.e., 0.5 % in this study) to stop the analysis should be investigated more thoroughly in future studies.

## CRediT authorship contribution statement

**Hoang D. Nguyen:** Writing – original draft, Validation, Methodology, Investigation, Formal analysis, Data curation, Conceptualization.

**Chanyoung Kim:** Writing – original draft, Formal analysis, Data curation. **Myoungsu Shin:** Writing – review & editing, Validation, Supervision, Methodology, Funding acquisition, Conceptualization.

## Declaration of competing interest

The authors declare that they have no known competing financial interests or personal relationships that could have appeared to influence the work reported in this paper.

## Acknowledgment

This research was supported by the Korea Institute of Energy Technology Evaluation and Planning (KETEP) grant funded by the Korean government (MOTIE) (Grant No. 20224B10300010), and the BK21plus Program (Grant No. 4299990613923) funded by the Ministry of Education and National Research Foundation of Korea.

## References

[1] S. Mishra, I. Thangamani, R.K. Singh, Containment leakage characterization with BARCOM test results for design and over pressure conditions, Nucl. Eng. Des. (2016), https://doi.org/10.1016/j.nucengdes.2016.03.004.
[2] S. Alhanaee, Y. Yi, A. Schiffer, Ultimate pressure capacity of nuclear reactor containment buildings under unaged and aged conditions, Nucl. Eng. Des. (2018), https://doi.org/10.1016/j.nucengdes.2018.05.017.
[3] Y.-S. Choun, H.-K. Park, Containment performance evaluation of prestressed concrete containment vessels with fiber reinforcement, Nucl. Eng. Technol. 47 (2015) 884–894, https://doi.org/10.1016/j.net.2015.07.003.
[4] B. Ghanbari, M. Fathi, A.H. Akhaveissy, Fragility curves for reinforced concrete (RC)/steel vertical hybrid frame structure under mainshock–aftershock sequences, J. Struct. Integr. Maint. (2023), https://doi.org/10.1080/24705314.2023.2220946.
[5] X. Huang, O.S. Kwon, E. Bentz, J. Tcherner, Evaluation of CANDU NPP containment structure subjected to aging and internal pressure increase, Nucl. Eng. Des. (2017), https://doi.org/10.1016/j.nucengdes.2017.01.013.
[6] H.T. Hu, Y.H. Lin, Ultimate analysis of PWR prestressed concrete containment subjected to internal pressure, Int. J. Press. Vessel. Pip. (2006), https://doi.org/10.1016/j.ijpvp.2006.02.030.
[7] H.T. Hu, J.X. Lin, Ultimate analysis of PWR prestressed concrete containment under long-term prestressing loss, Ann. Nucl. Energy (2016), https://doi.org/10.1016/j.anucene.2015.10.005.
[8] S. Wang, Analytical evaluation of the dome-cylinder interface of nuclear concrete containment subjected to internal pressure and thermal load, Eng. Struct. (2018), https://doi.org/10.1016/j.engstruct.2018.01.063.
[9] L. Zhou, J. Li, H. Zhong, G. Lin, Z. Li, Fragility comparison analysis of CPR1000 PWR containment subjected to internal pressure, Nucl. Eng. Des. (2018), https://doi.org/10.1016/j.nucengdes.2018.02.005.
[10] S. Jin, J. Gong, Fragility analysis and probabilistic performance evaluation of nuclear containment structure subjected to internal pressure, Reliab. Eng. Syst. Saf. (2021), https://doi.org/10.1016/j.ress.2020.107400.
[11] S. Jin, Z. Li, Z. Dong, T. Lan, J. Gong, A simplified fragility analysis methodology for containment structure subjected to overpressure condition, Int. J. Press. Vessel. Pip. (2020), https://doi.org/10.1016/j.ijpvp.2020.104104.
[12] H.D. Nguyen, C. Kim, Y.-J. Lee, M. Shin, Incorporation of machine learning into multiple stripe seismic fragility analysis of reinforced concrete wall structures, J. Build. Eng. 97 (2024) 110772, https://doi.org/10.1016/j.jobe.2024.110772.
[13] H.D. Nguyen, M. Shin, M. Torbol, Reliability assessment of a planar steel frame subjected to earthquakes in case of an implicit limit-state function, J. Build. Eng. 32 (2020), https://doi.org/10.1016/j.jobe.2020.101782.
[14] H.D. Nguyen, M. Shin, Effects of soil–structure interaction on seismic performance of a low-rise R/C moment frame considering material uncertainties, J. Build. Eng. 44 (2021) 102713, https://doi.org/10.1016/j.jobe.2021.102713.
[15] S. Ghavamian, A. Courtois, J.L. Valfort, Mechanical simulations of SANDIA II tests OECD ISP 48 benchmark, Nucl. Eng. Des. (2007), https://doi.org/10.1016/j.nucengdes.2006.10.012.
[16] G.P. Balomenos, M.D. Pandey, Probabilistic finite element investigation of prestressing loss in nuclear containment wall segments, Nucl. Eng. Des. (2017), https://doi.org/10.1016/j.nucengdes.2016.11.018.
[17] I. Hahm, D. Park, H.K. Choi, Probabilistic Ultimate Pressure Capacity Evaluation of PWR Type Containment Buildings, KAERI, 2014.
[18] A.H. Barbat, M. Cervera, A. Hanganu, C. Cirauqui, E. Oñate, Failure pressure evaluation of the containment building of a large dry nuclear power plant, Nucl. Eng. Des. (1998), https://doi.org/10.1016/S0029-5493(97)00329-4.
[19] International Atomic Energy Agency (IAEA), Status Report 83 - Advanced Power Reactor 1400 MWe (APR1400), 2011.
[20] D.S. Simulia, Abaqus 6.14, Abaqus 6.14 Anal. User's Guid, 2014.
[21] B. Alfarah, F. López-Almansa, S. Oller, New methodology for calculating damage variables evolution in Plastic Damage Model for RC structures, Eng. Struct. (2017), https://doi.org/10.1016/j.engstruct.2016.11.022.
[22] M. Mansour, T.T.C. Hsu, Behavior of reinforced concrete elements under cyclic shear. II: theoretical model, J. Struct. Eng. (2005), https://doi.org/10.1061/(asce)0733-9445(2005)131:1(54).
[23] Regulatory Guide 1, 216, Containment structural integrity evaluation for internal pressure loadings above design-basis pressure, Nucl. Regul. Comm. (2010).
[24] H. Kwak, Y. Kwon, Structural Integrity Assessment of a Reactor Building under Beyond-Design-Basis Internal Pressure and Temperature Conditions, KAIST, Daejeon, South Korea, 2012.
[25] M.R. Rajashekhar, B.R. Ellingwood, Reliability of reinforced-concrete cylindrical shells, J. Struct. Eng. (1995), https://doi.org/10.1061/(asce)0733-9445(1995)121:2(336).